Chapter

# Torque Ripple Reduction in DTC Induction Motor Drive

*Adhavan Balashanmugham, Maheswaran Mockaisamy and Sathiyanathan Murugesan*

## Abstract

The asynchronous or Induction Motor (IM) is one of the most widely used electrical machines in the world, due to the three following advantages namely 1. Their construction is simple and rugged 2.The absence of slip rings, commutators and brushes make it cheaper, and 3.It is also maintenance free compared to DC motors and Synchronous motor due to wear and tear of brushes, slip rings and commutators respectively. The Section 1 deals with the introduction of induction motor and Direct Torque Control scheme. Section 2 briefly discusses the types of Induction motor. Section 3 tells about the control strategies of Induction motor respectively scalar control and vector control, and also briefly explains about Direct Torque Control (DTC) method. The Section 4 discuss about the Types of Control Strategies for Torque ripple Reductions in DTC as well as the two proposed schemes namely 1.Fuzzy Logic Controller (FLC) for DTC-SVM and 2.Artificial Neural Network (ANN) controller for DTC-SVM respectively for IM and its results, The two proposed schemes uses Hybrid Asymmetric Space Vector Pulse Width Modulation (HASVPWM) for switching the inverter. The Section 5 revels about the modern advanced techniques such as ANN and FLC based DTC.

**Keywords:** types of IM, control techniques of IM, direct torque and flux control (DTC), torque ripple reductions in DTC, modern strategies of DTC, fuzzy logic controller (FLC) for DTC-SVM, artificial neural network (ANN) controller for DTC-SVM, hybrid asymmetric space vector pulse width modulation (HASVPWM)

## 1. Introduction

The electric motors are electromechanical machines, which are used for the conversion of electrical energy into mechanical energy. The foremost categories of AC motors are asynchronous and synchronous motors. The asynchronous motors are called singly excited machines, that is, the stator windings are connected to AC supply whereas the rotor has no connection from the stator or to any other source of supply. The power is transferred from the stator to the rotor only by mutual induction, owing to which the asynchronous motors are called as induction machines. The induction motor is used widely in several industrial applications because of the following advantages 1. Ruggedness 2. Good efficiency 3. Simple and easy control. When the induction motor is compared to separately excited DC drives it is inferior because of coupled torque and flux. To bring high performance in induction motor drive the advanced control techniques of induction motor uses independent control of torque and flux, like in separately excited DC drives.

The advanced control techniques such as field oriented control and direct torque control play vital role in today's high performance AC drives. Later in the 1980s, the direct torque control (DTC) method was proposed by Takahashi and Depenbrock [1, 2]. The direct torque control is a robust method compared to other methods. In this method by selecting optimum inverter switching modes the motor torque and flux are controlled independently and also direct. The primary input of the motor is stator voltage and stator current. From this the stator flux and electromagnetic torques are calculated. The torque errors and flux errors are limited within the hysteresis band. The Direct torque control of induction motors based on discrete space vector modulation using adaptive sliding mode control was proposed by Ben Salem and Derbel [3], the results shows the effectiveness and the robustness of the DTC- discrete SVM adaptive sliding mode control of induction motors. The variations of induction motor parameters is shown by Ben Salem and Derbel in their subsequent two publications namely Performance Analysis of DTC-SVM Sliding Mode Controllers-Based on Estimator of Electric Motor Speed Drive [4], and DTC-SVM Based Sliding Mode Controllers with Load Torque Estimators for Induction Motor Drives [5] respectively. The advantages of this direct torque control method is improved efficiency and fast response of torque in dynamic conditions [6, 7].

## 2. Types of induction motor

A typical three phase Induction motor consists of two parts namely stator and rotor, the outer part is called stator having coils supplied with three phase AC current to produce a rotating magnetic field. The inside rotating part is called rotor attached to the output shaft that is gives the useful torque produced by the rotating magnetic field. The stator is made up of stack of steel laminations of 0.35-o.5 mm thick with slots similar to a stator of a synchronous machine. The Coils are placed in the slots to form a three or single phase winding. **Figure 1A** shows the stator stampings with slots of induction motor **Figure 1B** shows the stator of induction motor [6].

The rotors of induction motors are of two types namely squirrel cage rotor and slip ring rotor. The squirrel cage rotor is made up of punched laminations with (0.35 to 0.5) mm thick steel core with rotor slots. Aluminum bars are molded in the slots instead of winding. End rings short circuit the aluminum bars at each side [6]. **Figure 2** shows the squirrel cage rotor.

The slip ring rotor or wound rotor has windings like the stator and at the end of each phase the winding is connected to a slip ring. There are three slip rings and

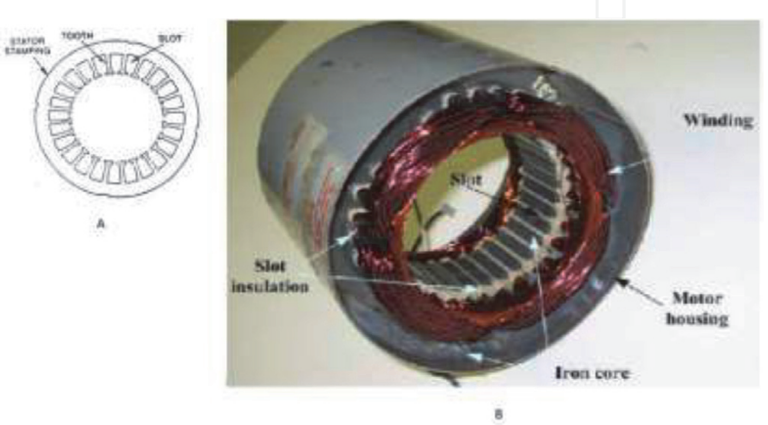


**Figure 1.**
*(A) Stator stamping with slots of induction motor. (B) Stator of Induction Motor.*

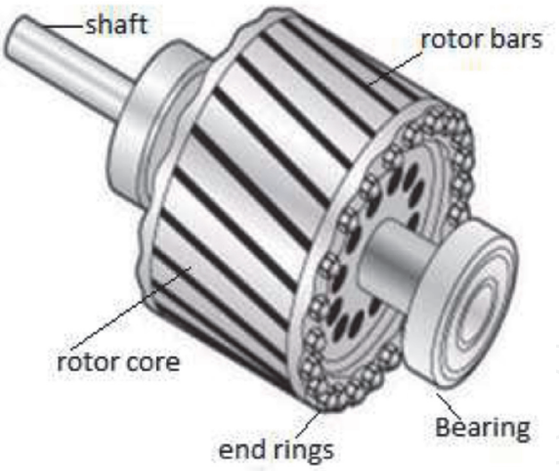


**Figure 2.**
*Squirrel cage rotor.*

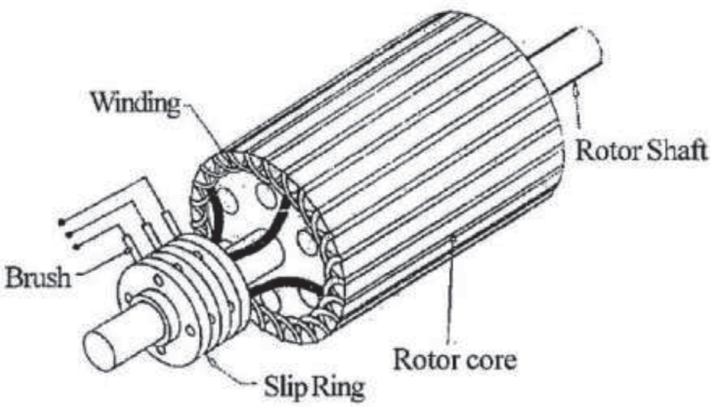


**Figure 3.**
*Slip ring rotor.*

three brushes through which three resistances can be connected in three phase star configuration for reducing starting current and speed control as well as increasing the torque [6]. **Figure 3** shows the slip ring rotor.

## 3. Classification of IM control strategies

The various IM control techniques are classified in to scalar and vector control methods. The general classification of IM control strategies [8, 9] which are based on the variable frequency control is shown in **Figure 4**.

### 3.1 Scalar control

The various scalar control methods are as follows 1. Stator voltage control 2. frequency control 3. Voltz/Hertz (V/F) control 4. Rotor Voltage control 5. Changing the number of poles. Out of these scalar methods, V/F control method is the best scalar control method. It can able to adjust the speed of the Induction motor by controlling the amplitude and frequency of the stator voltage of induction motor, the ratio of stator voltage to frequency should be kept constant so that, it is called as V/F control of induction motor drive. The vector control is preferred over scalar control methods due to the following disadvantages of scalar methods 1. Control of

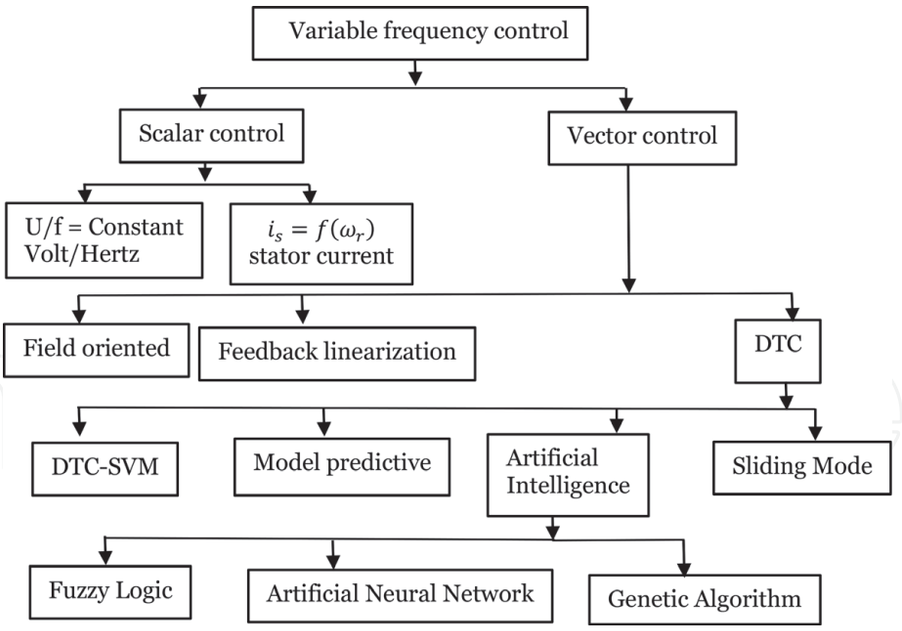


**Figure 4.**
*General classification of control strategies of induction motor.*

Voltage/Current/frequency magnitude is based on steady state equivalent circuit model which ignores transient conditions. 2. Coupling of torque and flux exists, and they are functions of frequency and voltage which leads to sluggish dynamic responses [6].

## 3.2 Vector control methods

### *3.2.1 Field oriented control (FOC)*

The FOC method is implemented based on the analogy of controlling a DC motor. It does not guarantee an exact decoupling of the torque and flux in dynamic and steady state operations. The full information about motor state variable and load torque is required for controlling the IM. The relationship between regulated value and control variables is linear only for constant rotor flux amplitude. The current controllers, coordinate transformations and a PWM algorithm are required. For direct FOC, flux estimator is required. In indirect FOC mechanical speed sensor is needed. This method is very sensitive to rotor time constant.

### *3.2.2 Direct torque control (DTC)*

The DTC is one of the high performance control strategies for the control of AC machine. In a DTC drive applications, flux linkage and electromagnetic torque are controlled directly and independently by the selection of optimum inverter switching modes of operation. To acquire a faster torque output, low inverter switching frequency and low harmonic losses in the model, the selection is made to restrict the flux linkages and electromagnetic torque errors within the respective flux and torque hysteresis bands. The required optimal switching vectors can be selected by using the optimum switching voltage vector look-up table. This can be obtained by simple physical considerations involving the position of the stator-flux linkage space vector, the available switching vectors, and the required torque flux linkage.

The torque is controlled by the stator current component $I_{sq}$ in the classical vector control strategy of FOC according to the Eq. (1)

$$M_e = p_b \frac{m_s}{2} \frac{L_M}{L_r} \Psi_r I_{sq} \tag{1}$$

The motor torque is expressed by rotor flux magnitude $\Psi_r$ and stator current component $I_{sq}$ as given in the Eq. (2) and this equation is written as:

$$M_e = p_b \frac{m_s}{2} \frac{L_M}{L_r} \Psi_r I_s sin\delta \tag{2}$$

The Eq. (2) is transformed into the Eq. (3)

$$M_e = p_b \frac{m_s}{2} \frac{L_M}{L_r L_s - L_m{}^2} \Psi_s \Psi_r \ sin\,\delta_\Psi \tag{3}$$

where $\delta$ is the angle between rotor flux vector and stator current vector and $\delta_\Psi$ is the angle between rotor and stator flux vectors. The torque value depends on the magnitude of stator and rotor flux as well as the angle $\delta_\Psi$. For FOC methods, the angle $\delta$ is considered whereas angle $\delta_\Psi$ is considered for DTC techniques.

The vector diagram of IM is shown in **Figure 5**.

From the motor voltage Eq. (5) for the omitted voltage drop on the stator resistance, the stator flux can be expressed.

From the mathematical model of IM, the electromagnetic torque equation is given in the Eq. (4)

$$M_e = p_b \frac{m_s}{2} \ Im\left(\Psi_s^* I_s\right) \tag{4}$$

Taking into consideration the fact that in the cage motor the rotor voltage equals zero and the electromagnetic torque Eq. (4), the following Eq. (5) is derived.

$$U_{sK} = R_s I_{sK} + \frac{d\Psi_{sK}}{dt} + j\Omega_K \Psi_{sK} \tag{5}$$

$$\frac{d\Psi_s}{dt} = U_s \tag{6}$$

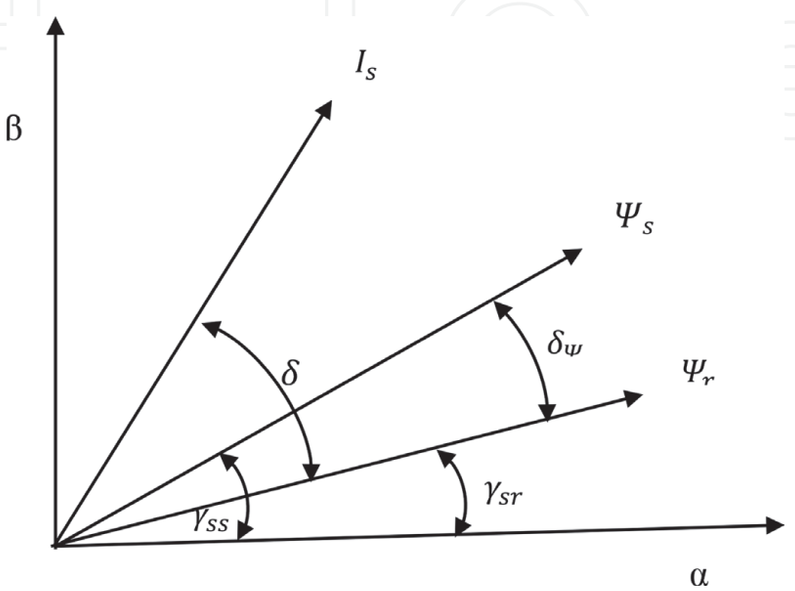


**Figure 5.**
*Vector diagram of induction motor.*

Taking into consideration the output voltage of the inverter in the above Eq. (6) it can be written as

$$\Psi_s = \int_0^t U_v dt \tag{7}$$

where

$$U_v = \begin{cases} \frac{2}{3} U_{dc} e^{j(v-1)\pi/3} & v = 1 \dots 6 \\ 0, \dots \dots \dots \dots \dots \dots & v = 0, 7 \end{cases} \tag{8}$$

The Eq. (7) describes eight voltage vectors which correspond to possible inverter states. These vectors are shown in **Figure 6**. There are six active vectors U1 to U6 and two zero vectors U0, U7.

It can be seen from the Eq. (7) that the stator flux directly depends on the inverter voltage Eq. (8). By using one of the active voltage vectors the stator flux vector moves to the direction and sense of the voltage vector. Stator flux changes direction for the cycle sequence of the active voltage vectors. Inherently the rotor flux of IM moves slowly but the stator flux could be changed immediately. In DTC methods the angle $\delta_\Psi$ between stator and rotor flux is varied to control the torque. By adjusting the stator voltage, stator flux could be controlled in simple way. The above consideration and equations could be used in the analysis of classical DTC techniques and SVM-DTC methods. In the classical DTC method the control plane is divided for the six sectors shown in **Figure 7**, that are defined as:

$$\gamma_{ss} \in \left(-\frac{\pi}{6}, +\frac{\pi}{6}\right) \tag{9}$$

$$\gamma_{ss} \in \left(+\frac{\pi}{6}, -\frac{\pi}{2}\right) \tag{10}$$

$$\gamma_{ss} \in \left(+\frac{\pi}{2}, +\frac{5\pi}{6}\right) \tag{11}$$

$$\gamma_{ss} \in \left(+\frac{5\pi}{6}, -\frac{5\pi}{6}\right) \tag{12}$$

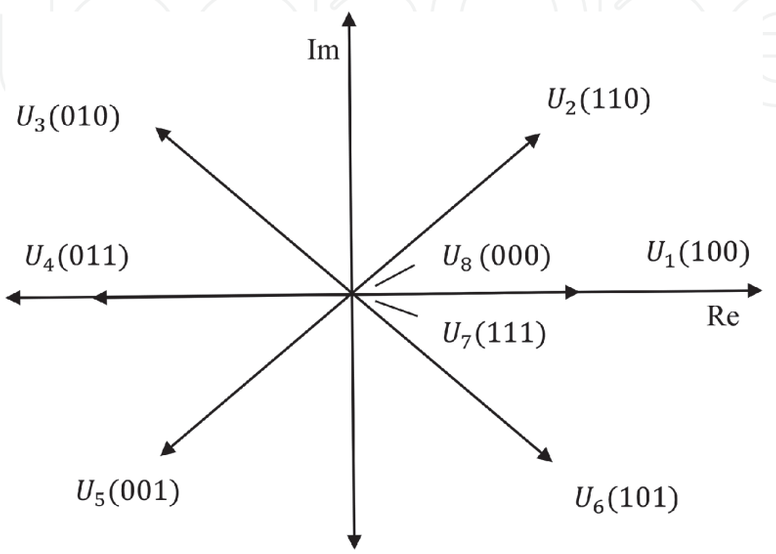


**Figure 6.**
*Inverter output voltage represented as space vectors.*

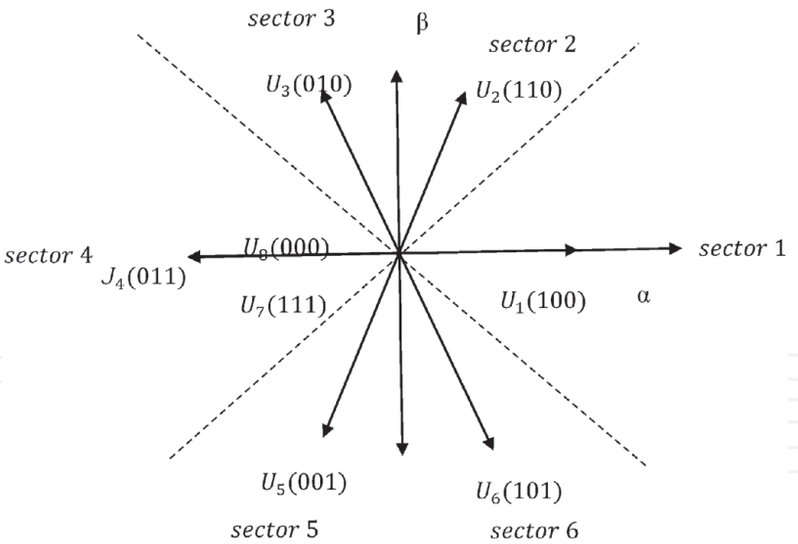


**Figure 7.**
*Sectors in classical DTC.*

$$\gamma_{ss} \in \left(-\frac{5\pi}{6}, -\frac{\pi}{2}\right) \tag{13}$$

$$\gamma_{ss} \in \left(-\frac{\pi}{2}, -\frac{\pi}{6}\right) \tag{14}$$

In order to increase magnitude of the stator vector in sector 1, the following voltage vectors $\mathbf{U_1}$ $\mathbf{U_2}$ $\mathbf{U_6}$ are selected. Conversely to decrease, $\mathbf{U_3}$ $\mathbf{U_4}$ $\mathbf{U_5}$ are selected. The stator flux is not changed when any one of the zero vectors $\mathbf{U_0}$ or $\mathbf{U_7}$ is applied. The solving of integration in Eq. (7) is stopped.

To increase the motor torque, the voltage vectors $\mathbf{U_2}$ $\mathbf{U_3}$ $\mathbf{U_4}$ are selected and for decreasing the torque $\mathbf{U_1}$ $\mathbf{U_5}$ $\mathbf{U_6}$ are selected. The switching **Table 1** is constructed based on the above considerations.

I. Takahashi and T. Nogouchi proposed the control scheme for Direct torque control and it is block diagram is shown in **Figure 8**.

The reference signals such as stator flux amplitude $\Psi_{sc}$ and the electromagnetic torque $M_c$ are compared with the estimated flux amplitude $\hat{\Psi}_s$ and electromagnetic torque $\hat{M}_e$ values respectively. The error values such as $e_\Psi$ and torque $e_M$ are sent to the hysteresis controllers. The appropriate voltage vector from the switching table is selected by the digitized output variables $d_\Psi$, $d_M$ and the stator flux position sector $\gamma_{ss}(N)$. The power switches in the inverter are controlled by the pulses $S_A$, $S_B$, $S_C$ which are generated form the switching table.

According to the Eq. (15) the torque and flux errors are calculated.

| $S_\Psi$ | $S_m$ | $S_1$ | $S_2$ | $S_3$ | $S_4$ | $S_5$ | $S_6$ |
|---|---|---|---|---|---|---|---|
| 1 | 1 | $U_2$ | $U_3$ | $U_4$ | $U_5$ | $U_6$ | $U_1$ |
| | 0 | $U_7$ | $U_0$ | $U_7$ | $U_0$ | $U_7$ | $U_0$ |
| | −1 | $U_6$ | $U_1$ | $U_2$ | $U_3$ | $U_4$ | $U_5$ |
| 0 | 1 | $U_3$ | $U_4$ | $U_5$ | $U_6$ | $U_1$ | $U_2$ |
| | 0 | $U_0$ | $U_7$ | $U_0$ | $U_7$ | $U_0$ | $U_7$ |
| | −1 | $U_5$ | $U_6$ | $U_1$ | $U_2$ | $U_3$ | $U_4$ |

**Table 1.**
*Optimum switching table.*

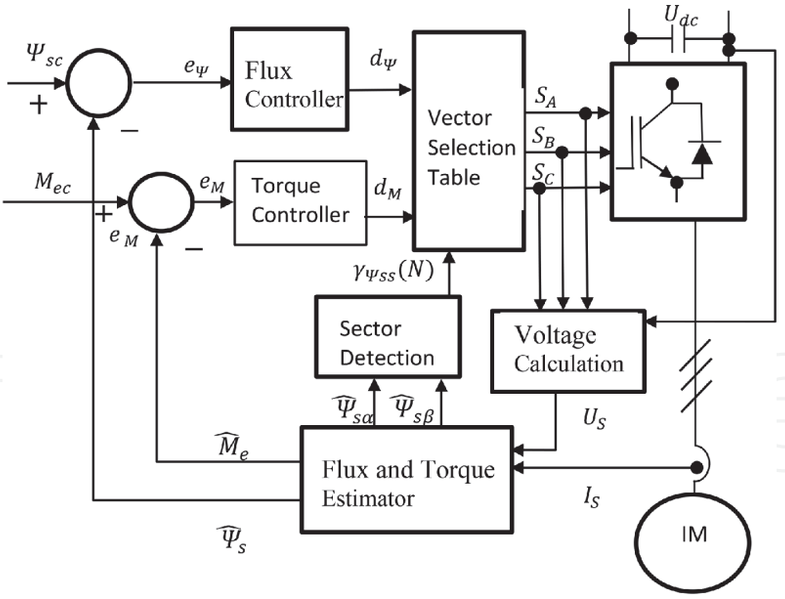


**Figure 8.**
*Block diagram of DTC scheme.*

$$\varepsilon_{\Psi_s} = \frac{\hat{\Psi}_s - \Psi_{sc}}{\Psi_{sN}} 100\% \tag{15}$$

*3.2.3 Problems in conventional DTC*

Despite its simplicity and robustness, the conventional DTC control has major drawback. The use of hysteresis controllers causes high ripples in the flux and electromagnetic torque at low speeds. It results in undesirable mechanical vibrations and acoustic noise, and subsequently leads to degradation of the machine performances. Thus the variable switching frequency and current distortions could detoriate the quality of the output power. The negligence in the calculation of stator resistance leads to problems at low speed. Moreover, the practical implementation of nonlinear components of the hysteresis type needs low sampling period. Many DTC strategies are developed based on the principle of instantaneous torque and stator flux regulation in order to rectify the drawbacks of classical DTC. The direct determination of the inverter control signals from the switching table is implemented [9].

## 4. Types of control strategies for torque ripple reductions in DTC

The DTC control strategies are divided into two groups: 1.Typical 2.Modern control strategies. They are classified into few other control techniques such as space vector modulation (SVM-DTC), modified switching table (m-DTC), Artificial Neural Network controller based (ANN-DTC), Fuzzy Logic controller based (FLC-DTC), Genetic algorithm based (GA-DTC), Model predictive controller based (MPC-DTC), Sliding mode based (SMO-DTC) [9, 10] as shown in **Figure 9**.

### 4.1 Modified DTC

It covers modification in switching table and/or injection of dithering signals. Few attempts are made to avoid the drawbacks in convention DTC either by implementing dither signal injection method or modified switching table method.

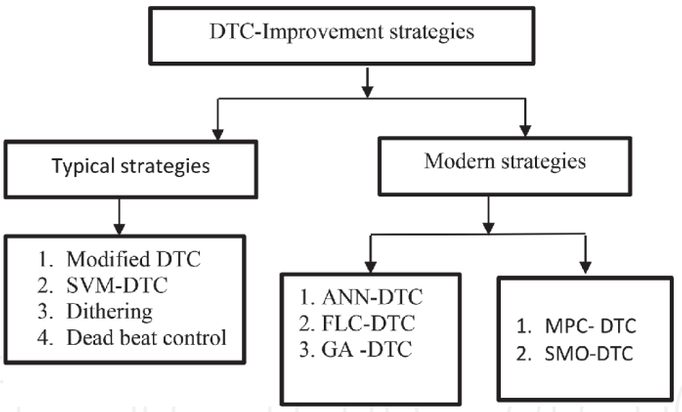


**Figure 9.**
*Classification of DTC improvement strategies.*

### *4.1.1 Modification in switching tables*

The modifications are carried out in the DTC- basic switching table with the objective of improving starting and overload conditions which enable all the voltage vectors are applied in appropriate sequence. They are implemented by two methods namely 1. Six sector table and 2. Twelve sector table respectively. The zero voltage vectors are selected from the switching **Table 1** during starting and very low speed conditions and results in flux level reduction due to the drop in stator resistance [11].

#### *4.1.1.1 Modified switching table*

##### *4.1.1.1.1 Improvement in switching table*

In conventional DTC, the states v1 and v4 vectors are not used. Depending on if the position is in its first 39 degrees or in its second ones, they could increase or decrease the torque. It leads to modify the switching table and use the modified DTC. In the modified DTC, the vectors v3 and v6 are not used. The reason is the ambiguity in flux instead of torque as if it was in conventional DTC [12].

##### *4.1.1.1.2 Modified classical DTC*

By applying zero voltage vectors V0, V7 for the states of decreasing in torque, **Table 1** is modified accordingly. The inertia of the motor is reduced when zero voltage vectors are applied, torque ripple is reduced. It is more suitable than the percent given by applying the voltage vectors in **Table 1** for the torque decrease states. **Table 2** illustrates this modification [12].

| Voltage vectors | Classical DTC | DTC with changes of zones |
|---|---|---|
| $V_1$ | +30° to −30° | 0° to −60° |
| $V_2$ | +90° to +30° | +60° to 0° |
| $V_3$ | +150° to +90° | +120° to +60° |
| $V_4$ | −150° to +150° | +180° to +120° |
| $V_5$ | −90° to −150° | −120° to −180° |
| $V_6$ | −30°to −90° | −60° to −120° |

**Table 2.**
*Modified switching table with 6-sectors.*

In both classical DTC and modified DTC there are two states per sector that present a torque ambiguity, so they are never used either. Instead of six sectors, the stator flux locus is divided into twelve sectors. Then all six active states will be implemented per sector. Consequently, the idea of the twelve sector modified DTC [13] is introduced. The tangential voltage vector component is very small and consequently its torque variation will be small as well. Based on this fact, the technique of small torque increase instead of torque increase is implemented [10, 11].

### *4.1.2 Dither signal injection*

Feedback signals should not be delayed in order to maintain maximum possible switching frequency. Due the presence of isolation amplifier, Hall effect transducer and other components, the delay is made inevitably. By introducing the dither signal at very high frequency, the effect due to delay could be compensated. Normally these dither signals are triangular waves at double or triple the sampling frequency of the system. This dithering technique minimizes the torque ripple to 30% compared to conventional DTC method [14].

The frequency of the dither signal is selected well above the cutoff frequency of the system so that its presence could not be detected in the output. When the system parameters are not exactly known and not alterable, the method of instantaneous injection of dither signal is robust to noise in measurements. The inherent delay in signal transduction, data acquisition system and computation leads to low switching frequency which would result in increased torque and flux ripples. The dithering signal injection is implemented to improve the switching frequency of inverter. The appropriate magnitude and frequency of dither signals which are injected in torque and flux errors could minimize torque ripples and acoustic noise level in the drive [15].

### *4.1.3 Deadbeat control*

In the inverter operation to avoid a short circuit in the DC-link, only one switch is turned on at a time. During the transistor switching signals, a delay time must be inserted and as a result the transistors stops to conduct. The dead-time TD is presented for the transistors $T_1$, $T_2$ for the two control signals SA+, SA- respectively. Most of the transistors take 1-3 μs duration of dead-time. The safe operation of the inverter is guaranteed by this delay time but it results into a serious distortion in the output voltage. Consequently there is a loss of control momentarily, where a deviation in output voltage from the reference voltage is observed. It is repeated for every switching cycle, so it has significant impact on the control of the inverter and this is known as dead-time effect. The inverter has nonlinear characteristics due to the dead-time and voltage drop on the switching devices. So the compensation algorithms are required in the control strategies [8] as shown in **Figure 10**.

The dead-beat DTC scheme is based on the technique, forcing the magnitude of torque and stator flux to attain their reference values in one sampling period. It is achieved by synthesizing a suitable stator voltage vector applied from Space Vector Modulation (SVM). In this approach the changes in the magnitude of torque and flux over one sampling period are calculated from the motor equations. To get the command value of stator voltage vector in stationary coordinates, a quadratic equation is solved [11].

The flux estimation is crucial part in the sensor less control strategies. The algorithm used for this is sensitive on the calculation accuracy of the inverter output voltage. From the switching signals, the voltages are reconstructed. **Figure 11** shows

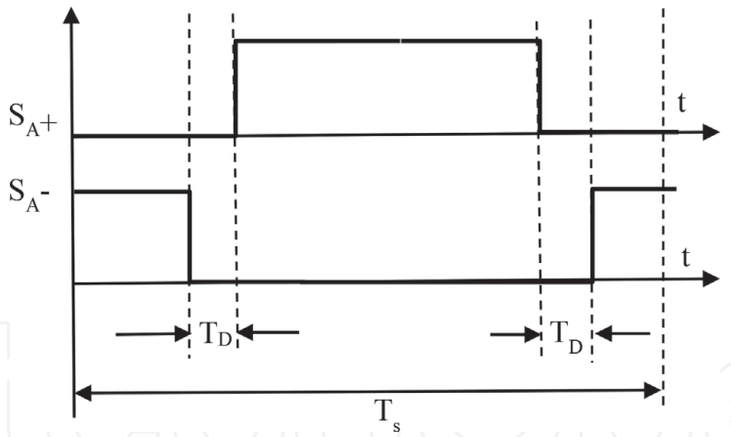


**Figure 10.**
*Dead-time effect in PWM inverter.*

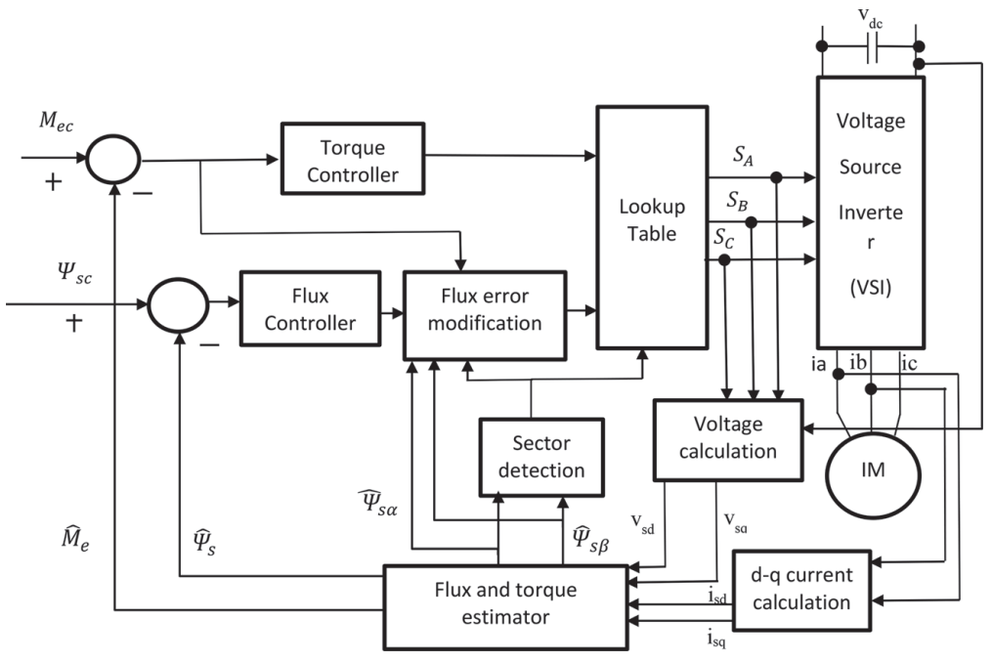


**Figure 11.**
*DTC control with modification of flux error status block.*

the DTC control with modification of flux error status block [13] dead-time compensation algorithm is significant in this SVM-DTC method [8].

The torque and flux ripple are reduced when the switching frequency of the inverter is maintained constant and greater than the sampling frequency [11].

### *4.1.3.1 Constant switching frequency approach*

For general purpose IM drives, PI-DTC is an appropriate solution in a very wide power range. It is suited to very fast torque and flux controlled drives because of its short sampling time which is required by the switching table DTC schemes [10].

The stator resistance influences the estimation accuracy of stator flux. The characteristics of both torque and flux control loops are affected by error in estimation of stator flux. A new strategy in MATLAB/SIMULINK model is implemented with modified flux error block which resulted in getting quick response [13].

The largest tangential vector to the circular flux locus is produced by an optimized voltage vector. This voltage vector is switched and held to achieve a fast rate

of change of angle Δδsr. The optimized voltage before being it is fed to the lookup table; its selection is done by modifying the flux error status [13].

### *4.1.4 SVM-DTC*

The main difference between classical DTC and DTC-SVM (**Figure 12**) control methods lies in which the control algorithm is being used for the calculations. Based on the instantaneous values, the classical DTC algorithm directly calculates the digital control signals for the inverter. In the DTC-SVM methods control algorithm calculations are based on averaged values whereas the switching signals for the inverter are calculated by space vector modulator. Based on voltage model, the flux estimator with reference flux is selected for the implementation DTC-SVM control structure in sensor less mode of operation [8].

#### *4.1.4.1 SVM*

The classical DTC has several disadvantages, among which the variable switching frequency and the high level of ripples are the prominent issues [16]. Further they lead to high-current harmonics and an acoustical noise and they detoriate the control performance at low speeds. The ripples are produced proportionally to the width of the hysteresis band. Due to the discrete nature of the hysteresis controllers, even for the reduced bandwidth values, the ripples are still present [16].

The inverter switching frequency is increased due to even very small values of bandwidths. The modifications in classical DTC strategy is done by including a vector modulator block, which produces space vector PWM technique (SVM) and it is used to implement the voltage vector with a fixed frequency of inverter switching. The switching table and hysteresis controllers are replaced with PI controllers to control the stator flux and the torque [13].

The disadvantages of DTC-SVM with conventional PI controllers are as follows 1. Sensitivity to variation in system parameters and 2. Inadequate rejection of external disturbances and 3. Load changing conditions. These disadvantages are overcome by replacing the conventional PI controllers by intelligent controllers such as adaptive fuzzy-PI or FLC. These intelligent controllers ol more robust against the external disturbances and parameter variations [13].

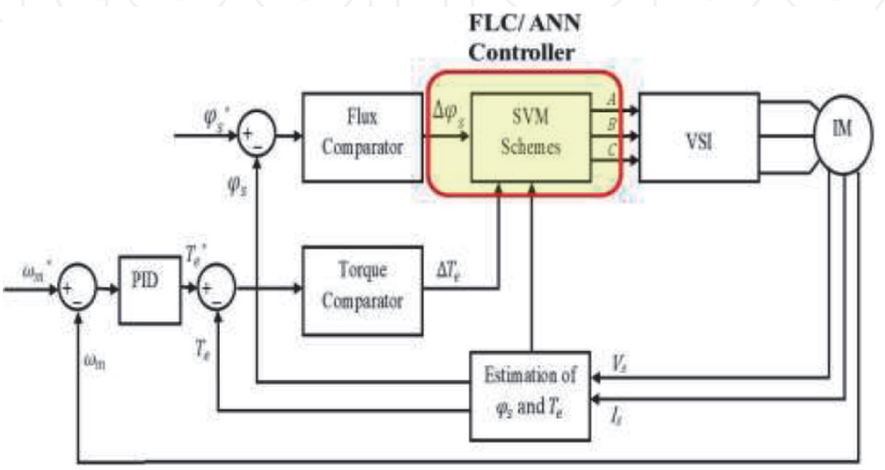


**Figure 12.**
*Block diagram of FLC/ANN controller for DTC-SVM scheme for induction motor.*

#### *4.1.4.2 Types of SVM-DTC*

The DTC-SVM methods have several following classes namely:

1. PI controllers based DTC-SVM.

2. Predictive/dead-beat based DTC-SVM.

3. Fuzzy logic and/or neural networks based DTC-SVM.

4. Variable-structure control (VSC) [8] based DTC-SVM.

The use of PI controller for torque control of induction motor drives is to overcome an overshoot during startup and to minimize steady state error. The PI controllers provide feedback signals to the system.

In voltage model based stator flux estimation, the pure integrator is replaced with LPF to eliminate the problem of saturation and integration drift due to the DC offsets which are present in the sensed currents or voltages. The LPF introduces the phase and magnitude errors of stator flux estimation which affects the selection of voltages vector and electromagnetic torque response, thereby it deteriorate the performance of DTC drive. To overcome the LPF problems, closed loop of stator flux estimation is implemented [17].

In MRAS, to estimate the rotor speed, PI controller is used and this controller takes more time to tune the proportional and integral gain to obtain the estimated target speed. The MRAS is based on rotor speed, rotor flux and stator current thereby it eliminates the need of PI controller [18].

The effective integration of SVM technique with any n-level multilevel inverter fed DTC drive is achieved by using a fractal based space-vector DTC algorithm. The current THD performance is improved at higher level of DTC drives under transient, steady state and speed reversal operating conditions. Without any significant modification, this strategy could be adapted at any n-level inverter fed DTC controller [19].

#### *4.1.4.3 Proposed artificial intelligent schemes for DTC-SVM*

The Space Vector PWM (SVPWM) is a technique used for solving the switching losses in the power converter. The SVPWM is operated in a symmetrical way, so the switching state of each sector is predefined. In this proposed scheme, the initial values to the DTC controller have been fixed based on the induction motor rating. Then the estimation of DTC parameters is found and it is fed to the reference to the Hybrid Asymmetric Space Vector PWM (HASVPWM) controller.

Traditional PWM techniques consist of two signals called carrier signal and reference signal for generating the PWM pulses. If any distortions in the reference signal (i.e error signal) may produce miscellaneous pulses, which will affect the performance of the converter. But SVPWM technique is purely based on estimating the voltage magnitude and its angle for pulse generation. In this, three phase voltages $V_{abc}$ are converted into $V_d$,$V_q$ and $V_0$ using abc-dq0 theory. This method will make the estimation of the sector angle and voltage magnitude easier. In traditional SVPWM, each sector denotes $60^0$ angles and totally it has six sector and two reference vector in its implementation. Even though the estimation is done for every sector accuracy of generating the pulses is lagging due to the higher range of sector angle and minimum switching sectors. For an example, if estimated sector angle is $55^0$, then the switching pattern in sector 1 is selected for the PWM generation. But $V_2$ vector is also having different switching pattern and that may also well

suited for the same estimated sector angle $55^0$. In order avoid such difficult situations, a HASVPWM is used for controlling the DTC drive which reduces torque ripples, switching losses and improved power quality.

The implementation of HASVPWM is similar to the SVPWM technique. In general, three phase Voltage source inverters (VSI) have eight distinct switching losses, where state 1 to 6 are active states, 0 and 7 are inactive switching states. In HASVPWM, asymmetric voltage vectors are represented as $V_{ni}$, $V_{nj}$ and $V_{nk}$ where n = 1,2,3,4,5,6 and four quadrants. HASVPWM has two non-zero vectors ($V_1$ and $V_2$) and two zero vectors ($V_0$ and $V_{24}$) in each vector will be used for the vector $15^0$. Hence this HASVPWM have 24 sectors and it is shown in **Figure 13**.

Major portion in HASVPWM is to removal of mismatching pulses which will be done by comparing the HASVPWM pulses with the traditional SVPWM pulse. The mismatching pulses are removed by calculating its rise time ($T_r$) and fall time ($T_f$) of the mismatching pulses with magnitude. Then the same magnitude of pulse with same instant is added. For mismatching pulse removal. This logic avoids the mismatching pulses in the output and reduce the switching losses in the VSI based DTC drive. In this proposed system, intelligent control methods such as Fuzzy Logic Control (FLC) and Artificial Neural Network (ANN) are utilized to find the suitable sector for continuous operation. They are also efficient than the classical control techniques which are utilized to find suitable sector for the continuous operation.

#### *4.1.4.3.1 Fuzzy logic controller for HASVPWM*

The proposed hybridization process is performed by the combination of continuous ASVPWM and fuzzy operated Discontinuous ASVPWM technique. Finally, the mismatching pulses of both PWM techniques are applied to control the inverter. Pulse mismatching technique helps to reduce the active region of the switch and achieve the optimal input pulse to the inverter. Pulse mismatching technique helps to reduce the active region of the switch and achieve the optimal input pulse to the inverter. The optimal hybrid pulse reduces transition time of inverter switch and improves operating performance of the inverter. The Fuzzy rules help to select the optimal switching sector for discontinuous modulation. If there is more number of sectors in the hexagon, it allows more degrees of freedom which help to find the optimal reference voltage and angle. The Fuzzy logic system describes to what degree the rule applies, while the conclusion assigns a fuzzy function to each of one or more output variables. These Fuzzy Expert Systems allow more than one conclusion per rule.

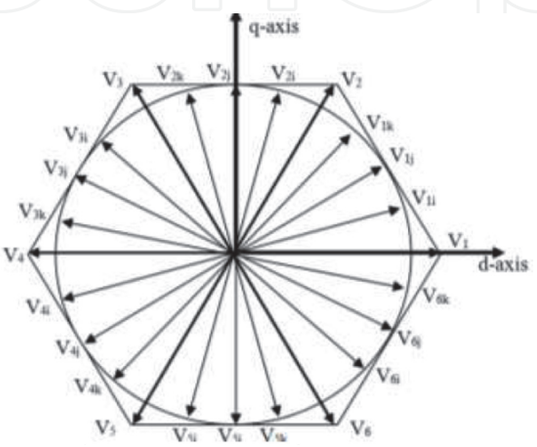


**Figure 13.**
*Structure of HASVPWM hexagon.*

| CE\E | NB | NS | ZE | PS | PB |
|---|---|---|---|---|---|
| **NB** | NB | NB | NS | NS | ZE |
| **NS** | NB | NS | NS | ZE | PS |
| **ZE** | NS | NS | ZE | PS | PS |
| **PS** | NS | ZE | PS | PS | PB |
| **PB** | ZE | PS | PS | PB | PB |

**Table 3.**
*Fuzzy Logic Rules to select suitable sector in HASVPWM.*

The linguistic labels are divided into five groups. They are: NB-Negative Big; NS- Negative Small; ZE-zero; PS-Positive Small; PB-Positive Big. Each of the inputs and the output contain membership functions with all these five linguistics.

The set of rules in a fuzzy expert system is given in **Table 3** and corresponding input and membership function values are indicated in **Figure 8**.

The simulation model of DTC with HASVPWM scheme is developed using MATLAB software Simulink tool. The fuzzified inputs and defuzzified outputs are shown in **Figures 14–16** respectively. Consider a case, when the sector angle estimated from the SVPWM calculation as shown in **Figure 14** is equal to $-165^0$, it means negative big (NB) as mentioned in **Table 3**. And change in the sector angle at the next instant is about $-110^0$, it represent the negative small (NS). Then the corresponding fuzzy output is NB, which is mentioned in **Figure 16**.

*4.1.4.3.2 Artificial neural network controller for HASVPWM*

The DTC control can also be achieved with HASVPWM using Artificial Neural Network (ANN) control. ANN is nonlinear model that is easy to use and understand compared to statistical methods like Fuzzy logic. Compare with Fuzzy Logic, ANN has an ability to learn from the previous trained data. Hence, the major advantage of

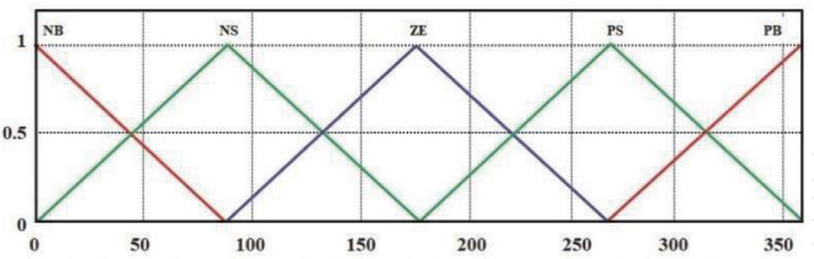


**Figure 14.**
*Degree input to FLC.*

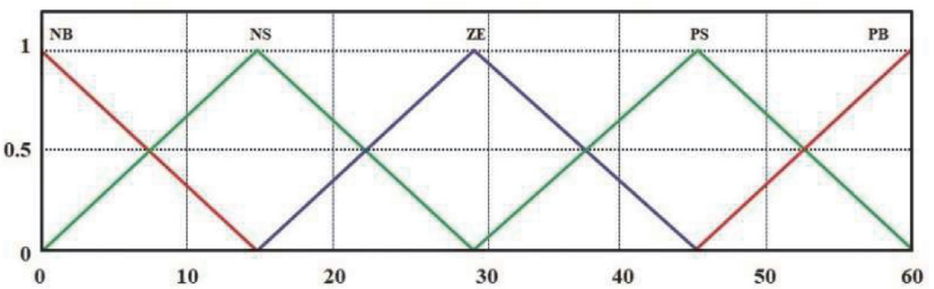


**Figure 15.**
*Change in degree error input to FLC.*

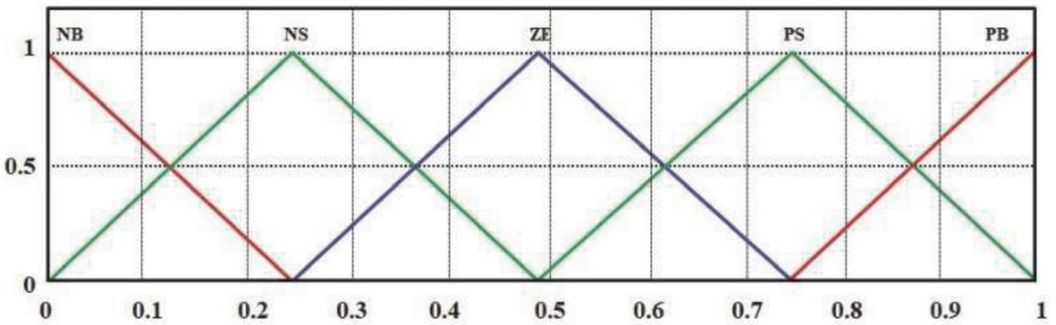


**Figure 16.**
*Fuzzy output Modulation index for HASPWM.*

ANN is to train a system with large amount of data sets. The output performance will depend upon the trained parameters and the data set relevant to the training data. In this proposed scheme, ANN is used to estimate the suitable sector of HASVPWM.

ANN is used to determine the sector number for the estimated value of θe. There are total of 24 sectors, each sector of 15 degree. Again three layers of neurons are used but with a 5–4-1 feed forward configuration as shown in **Figure 17**. The Input layer is of log sigmoid transfer function, hidden layer is of hyperbolic tangent sigmoid function and the output layer is of linear transfer function. Levenberg - Marquardt back propagation based training method is used for train the neurons. As soon as the training procedure is over, the neural network gives almost the same output pattern for the same or nearby values of input. This tendency of the neural networks which approximates the output for new input i.e. angle theta since sector selection is purely based on theta.

The following **Figure 17** shows the structure of Neural Network (NN) which is utilized in the proposed ANN controller for DTC-SVM scheme for induction motor.

The Step by step procedure for NN Algorithm is given below:

**Step 1:** Initialize the input weight for each neuron.

**Step 2:** Apply the training dataset to the network. Here X is the input to the Network and $Y_1$, $Y_2$ and $Y_3$ are the output of the network.

**Step 3:** Adjust the weights of all neurons.

**Step 4**: Determine Sector Angle for SVPWM.

Compare with Fuzzy logic control, ANN control in HASVPWM is able to identify the suitable voltage vector and its angle for minimizing the torque ripple and PEC losses and THD, maximizing DTC capabilities under various operating conditions like speed reversal, loading conditions etc. The effectiveness of ANN-HASVPWM in DTC scheme is predicted by comparing ANN with the Fuzzy based

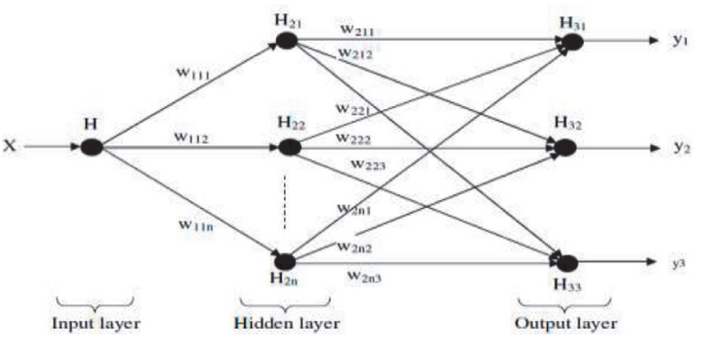


**Figure 17.**
*The structure of network utilized in the proposed technique.*

| Control strategies | Torque ripple factor (%) |
|---|---|
| Proposed FLC controller for HASVPWM FOR DTC-SVM scheme | **5.1** |
| Proposed ANN controller for HASVPWM FOR DTC-SVM scheme | **4.5** |

**Table 4.**
*Comparison of control strategies in induction motor.*

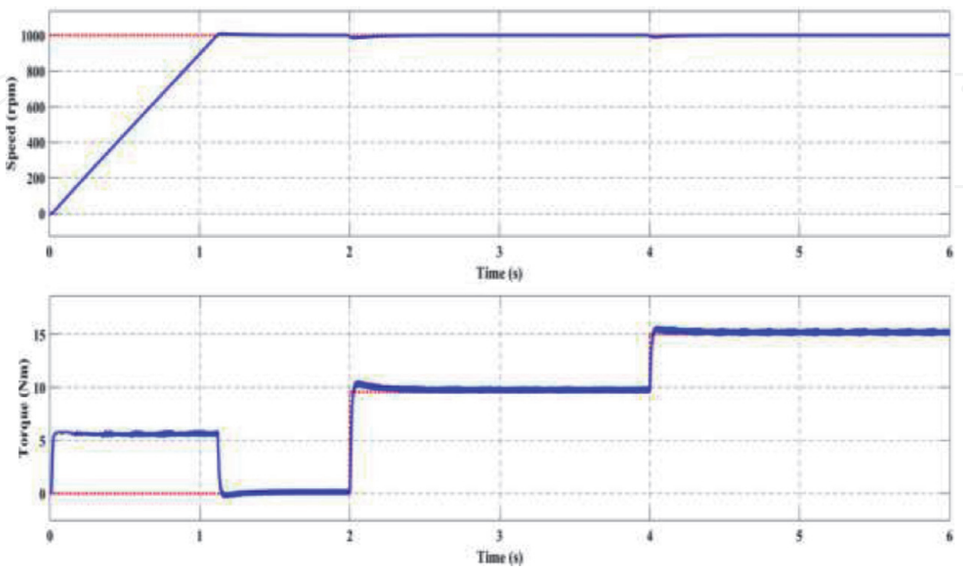


**Figure 18.**
*Speed and torque output for FLC based DTC-SVM of IM with HASVPWM.*

HASVPWM scheme. The results for ANN based HASVPWM scheme to DTC controller under the same loading conditions, it shows that torques ripple, switching loss and harmonic content reduction is expected. The comparative simulation results are clearly presented and shown in **Table 4**.

*4.1.4.3.3 Simulation results and discussion*

The two proposed schemes namely 1.Fuzzy Logic Controller (FLC) for DTC-SVM and 2.Artificial Neural Network (ANN) controller for DTC-SVM respectively for IM. Has been simulated using MATLAB version R2009a and the results are compared and shown in **Table 4**. Both of the proposed scheme methods uses HASVPWM. The parameters of IM used in the simulation are given in the appendix.

The torque ripple can be calculated by using the relation.

$$\text{Torque Ripple Factor} = (\text{Peak to Peak torque})/\text{Rated torque} \qquad (16)$$

The simulation results of FLC for DTC-SVM of IM with HASVPWM is shown in **Figures 18** and **19**.The simulation results of ANN for DTC-SVM of IM with HASVPWM is shown in **Figures 20** and **21**.

From **Figure 19** (Torque ripple waveform) it is inferred that the torque ripples oscillates from 9.5 Nm (Minimum) to 10.1 Nm (maximum) for the given Reference torque of 10 Nm.

Torque Ripple factor (%) as per Eq. 23 is given by = ((10.01–9.5)/10) × 100 = 0.51/10×100 = **5.1.**

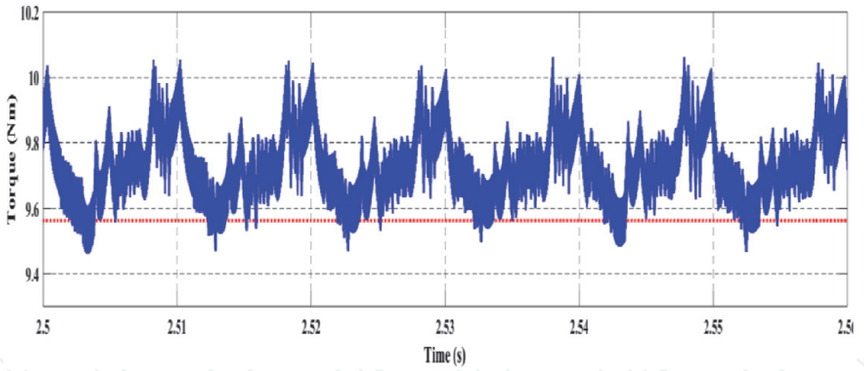


**Figure 19.**
*Torque ripples for FLC based DTC-SVM of IM with HASVPWM.*

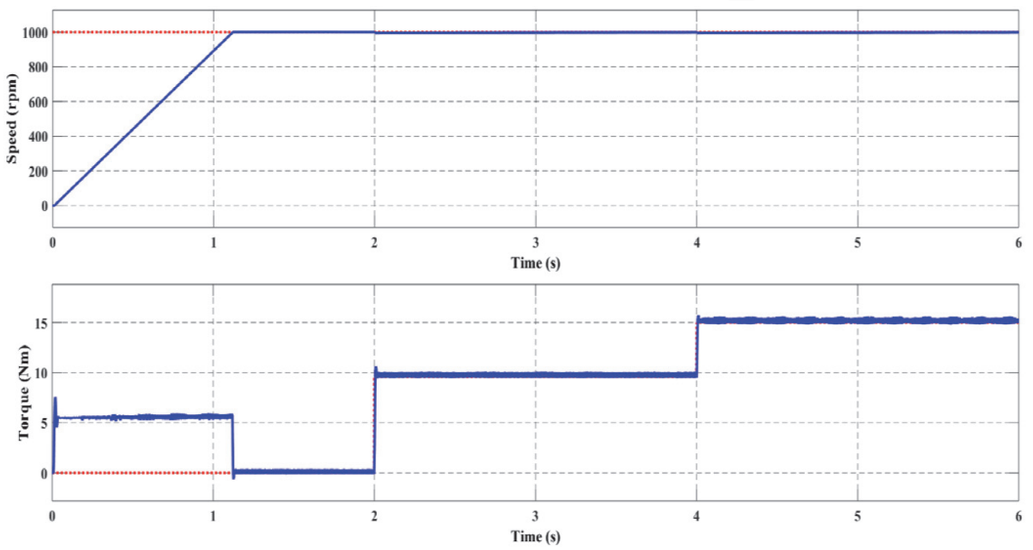


**Figure 20.**
*Speed and torque output for ANN based DTC-SVM of IM with HASVPWM.*

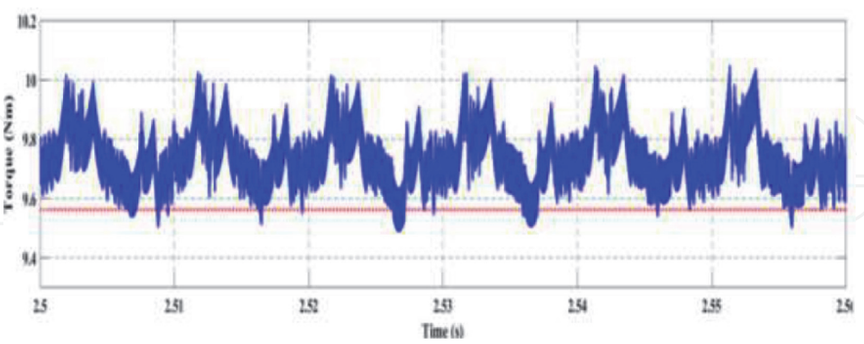


**Figure 21.**
*Torque ripples for ANN based DTC-SVM of IM with HASVPWM.*

From **Figure 21** (Torque ripple waveform) it is inferred that the torque ripples oscillates from 9.55 Nm (Minimum) to 10 Nm (maximum) for the given Reference torque of 10 Nm.

Torque Ripple factor (%) as per Eq. 23 is given by = ((10–9.55)/10) × 100 = 0.45/10×100 = **4.5.**

**Figure 22** shows the comparison of Torque Ripple of FLC and ANN based DTC-SVM of IM with HASVPWM at 1000 rpm.

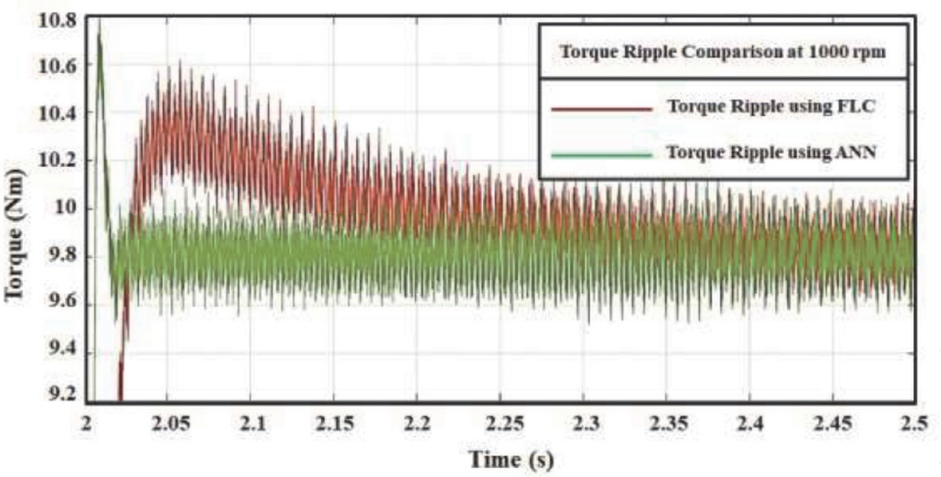


**Figure 22.**
*Torque ripple comparison of FLC and ANN based DTC- SVM of IM with HASVPWM.*

It is clear that variation in Torque ripples shown in **Table 4** is less in case of ANN and they can achieve a minimum torque ripple than other control techniques. It has been viewed that the discussed control strategy has helped in reducing the torque ripples. Thus, by using FLC and ANN based controller for DTC of IM, the ripples are reduced completely.

## 5. Modern strategies of DTC

### 5.1 Fuzzy logic control (FLC)

The limits of the torque hysteresis band are controlled by FLC. It entails a minimization of the torque ripples as well as an improvement of the dynamic performances of IM. The FLC selects the optimum bandwidth of the torque hysteresis in real time [9].

The fuzzified parameters such as torque error, stator flux errors, and stator flux angle are the input to FLC. The switching state of the inverter is a crisp value obtained as an output from the FLC [11].

A detailed classification and comparison of DTC strategies like SMC, FLC and ANN in terms of performance parameters of induction machine were discussed in [20].

The PI controller and FLC algorithm have been implemented for the three-phase induction motor and it is found that the proposed FLC scheme is better than the conventional DTC control with PI control in [21].

The effective DTC improvements are achieved by Fuzzy logic controller thereby the ripples in torque and flux are reduced, consequently secondary problems for the motor such as heating, mechanical vibration, aging are also rectified. The merits of the conventional are also preserved [22].

### 5.2 Artificial neural network (ANN)

A multilayer ANN allows to replace both hysteresis comparators and the selection table in classical DTC.

The ANN offers the following merit over classical DTC.

i. The complexity of the controller is reduced;

ii. The effects of motor parameter variations are minimized.

iii. The controller time response is improved.

iv. The robustness of drive is improved [11].

For electric vehicle applications, the FLC and ANN based monitoring systems for the DTC controlled induction motor drive was implemented to detect a very small change in performance parameters [23].

## Acknowledgements

We are thankful to the management of following institutes, the Department of Electrical and Electronics Engineering, PSG Institute of Technology and Applied Research, Coimbatore, Tamilnadu, India, and the Department of Mechatronics Engineering, Nehru Institute of Engineering and Technology, Coimbatore, India, for their encouragement, support and facilities provided for our book chapter work.

## Nomenclature

| | |
|---|---|
| $f_c$ | crossover frequency |
| $i_d$ | d-axis current |
| $L_{dm}$ | d-axis magnetizing inductance |
| $L_d$ | d-axis self-inductance |
| $V_d$ | d-axis voltage |
| $\rho$ | derivative operator |
| $T_e$ | develop electromagnetic torque |
| d | direct or polar axis |
| DTC | direct torque control |
| $\omega_r$ | electrical speed |
| $i_f$ | equivalent permanent magnet field current |
| $L_s$ | equivalent self-inductance per phase |
| $\lambda_d$ | flux linkage due d axis |
| $\lambda_q$ | flux linkage due q axis |
| $\lambda_{dm}$ | flux linkage due to rotor magnets linking the stator |
| B | friction |
| FLC | fuzzy logic controller |
| J | inertia |
| $k_i$ | integral control gain |
| $T_L$ | load torque |
| $\omega_{rated}$ | motor rated speed |
| $T_m$ | motor torque |
| P | number of poles |
| $I_m$ | peak value of supply current |
| $\lambda_f$ | PM flux linkage or field flux linkage |
| $k_p$ | proportional control gain |
| $i_q$ | q-axis current |
| $L_{qm}$ | q-axis magnetizing inductance |
| $L_q$ | q-axis self-inductance |
| $V_q$ | q-axis voltage |
| q | quadrature or interpolar axis |

| | |
|---|---|
| $T_{ref}$ | reference motor torque |
| $\theta_r$ | rotor position |
| $\omega_m$ | rotor speed |
| L | self-inductance |
| $L_{ls}$ | stator leakage inductance |
| $R_s$ | stator resistance |
| $i_a$, $i_b$, $i_c$ | three phase currents |
| $V_a$, $V_b$, $V_c$ | three phase voltage |

# A. Appendices

## A.1 Appendix 1: parameters of 3 phase squirrel cage induction motor

| | |
|---|---|
| RATED POWER | 5.4 HP |
| RATED VOLTAGE | 400 V |
| RATED SPEED | 1430 RPM |
| RATED TORQUE | 26.7 Nm |
| RATED CURRENT | 8.5 A |
| STATOR RESISTANCE | 1.405 Ω |
| ROTOR RESISTANCE | 1.395 Ω |
| STATOR INDUCTANCE Ls | 0.005839H |
| ROTOR INDUCTANCE Lr | 0.005839H |
| MAGNETIC FLUX | 0.1827 weber |
| NO. OF POLES | 4 |
| MOMENT OF INERTIA | 0.0131 $kgm^2$ |
| FRICTION FACTOR | 0.002985 Nms/rad |

## Author details

Adhavan Balashanmugham[1*], Maheswaran Mockaisamy[2] and Sathiyanathan Murugesan[1]

1 Department of Electrical and Electronics Engineering, PSG Institute of Technology and Applied Research, Coimbatore, Tamil Nadu, India

2 Department of Mechatronics Engineering, Nehru Institute of Engineering and Technology, Coimbatore, India

*Address all correspondence to: adhav14@gmail.com

## References

[1] Takahashi, Noguchi T. A new quick response and high-efficiency control strategy of an induction motor. IEEE Transactions on Industry Applications., Vol.22, No.5, pp.820–827, 1986. DOI: 10.1109/TIA.1986.4504799

[2] Depenbrock M. Direct self control (DSC) of inverter fed induction machine. IEEE Transactions on Power Electronics. 1988; 3(4):420–429. DOI: 10.1109/63.17963

[3] Ben Salem, F. and Derbel N., 'Direct torque control of induction motors based on discrete space vector modulation using adaptive sliding mode control', International Journal of Electric Power Components and Systems, 2014, 42, (14), pp. 1598–1610.

[4] F. Ben Salem and N. Derbel, 'Performance Analysis of DTC-SVM Sliding Mode Controllers-Based Parameters Estimator of Electric Motor Speed Drive', Mathematical Problems in Engineering, Volume 2014, Article ID 127128, http://dx.doi.org/10.1155/2014/127128, 2014.

[5] Ben Salem,F. and Derbel,N., 'DTC-SVM Based Sliding Mode Controllers with Load Torque Estimators for Induction Motor Drives', Chapter 14 of the Book: Applications of Sliding Mode Control, Studies in Systems, Decision and Control 79, Springer Science+ Business Media Singapore 2017, pp. 269–297

[6] P.C. Krause,O. Wasynczuk, S. D. Sudhoff "Analysis of Electric Machinery and Drive Systems", IEEE Press, A John Wiley & Sons, Inc. Publication Second Edition, 2002.

[7] H. C. Stanley, "An Analysis of the Induction Motor", AIEE Transactions, Vol. 57 (Supplement), pp. 751–755, 1938.

[8] Marcin Żelechowski. Space Vector Modulated – Direct Torque Controlled (DTC–SVM) Inverter–Fed Induction Motor Drive, Dissertation, Warsaw University of Technology; Warsaw, 2005. p. 1–175.

[9] Najib El Ouanjli et al. Modern improvement techniques of direct torque control for induction motor drives - a review. Protection and Control of Modern Power Systems. Springer Open; 2019. p. 1–12. https://doi.org/10.1186/s41601-019-0125-5.

[10] Vojkan Kostić et al. Expermental Verification of Direct Control Methods for Electric Drive Application. Facta Universitatis. Series: Automatic Control and Robotics; Vol. 8, No.1, 2009. pp. 111–126.

[11] M.Vasudevan. Improved Direct Torque Control Strategy with Ripple Minimization for Induction motor drive. Anna University: Chennai; 2006. p. 39–87.

[12] Eng.Ahmed Hassan Adel et al. Torque Ripple Reduction in Direct Torque Control of Induction Motor Drives by Improvement of the Switching Table. Journal of Multidisciplinary Engineering Science and Technology; Vol. 1 Issue 5, 2014. p. 1–6.

[13] Madhuri D. Kulkarni, Vivek D. Bavdhane. Quick Dynamic Torque Control in DTC-Hysteresis-Based Induction Motor by Using New Optimized Switching Strategy. International Journal of Innovations in Engineering Research and Technology; Vol. 2, Issue 7, 2015. p. 1–11.

[14] Jaya N. Tattea, Mohoda, S. B. Performance Improvement of Induction Motor by Using Direct Torque Control Technique. International Journal of Development Research; Vol. 07, Issue 10, 2017. pp.15901–15905.

[15] RK.Behra, SP.Das Improved direct torque control of induction motor with dither injection, Sadhana; Vol. 33, Part 5, 2008. p. 551–564.

[16] Cherifi Djamila, Miloud Yahia. Direct Torque Control Strategies of Induction Machine: Comparative Studies. Direct Torque Control Strategies of Electrical Machines. Intechopen p. 1–23. DOI: http://dx.doi.org/10.5772/intechopen.90199.

[17] Rajendran R. Certain Investigations and Realization of SVM-DTC of Induction Motor Drives Using FPGA. Anna University, Chennai; 2012. p. 46–66.

[18] Hassan Farhan Rashag et al. DTC-SVM Based on PI Torque and PI Flux Controllers to Achieve High Performance of Induction Motor. Research Journal of Applied Sciences, Engineering and Technology 7(4); 2014. p. 875–891.

[19] Vinod B. R., Shiny G. A Multilevel Inverter fed Direct Torque Control Strategy for an Induction Motor using PI Controllers. International Journal of Engineering and Advanced Technology; Volume-7 Issue-4, 2018. p. 90–99.

[20] Najib El Ouanjli et al. Modern Improvement Techniques of Direct Torque Control for Induction Motor Drives - A review, Protection and Control of Modern Power Systems. 2019, 4:11,https://doi.org/10.1186/s41601-019-0125-5, pp. 1–12.

[21] J. Jeyashanthi, M. Santhi. Performance of Direct Torque Controlled Induction Motor Drive by Fuzzy Logic Controller. CEAI; Vol.22, No.1, 2020, pp. 63–71.

[22] Najib El Ouanjli et al. Improved DTC strategy of doubly fed induction motor using fuzzy logic controller. Elsevier Energy Reports 5, 2019, pp. 271–279.

[23] Abarna J, Velnath R. Modeling of Three Phase Induction Motor with DTC Drive Fault Analysis using Fuzzy Logic. International Journal of Recent Technology and Engineering (IJRTE); ISSN: 2277–3878, Vol. 9, Issue-1, May 2020. pp. 1196–1202.